Paper No. 470. (quote when citing this article)
Eleventh World Conference on Earthquake Engineering
ISBN: 0 08 042822 3

TESTS AND ANALYSES OF HYBRID WALL SYSTEMS

T. KABEYASAWA, T. OHKUBO and Y. NAKAMURA

Earthquake Research Institute, University of Tokyo
Yayoi 1-1-1, Bunkyo-ku, Tokyo 113, Japan

ABSTRACT

Experimental and analytical studies on seismic design of hybrid wall system are reported conducted as a part of U.S.-Japan cooperative research program. The system consists of reinforced concrete coupled core walls and peripheral steel frames. Three T-shaped walls were tested under varying axial load to obtain the hysteretic behavior of the coupled core walls in different failure modes. The ultimate flexural and shear strengths were estimated theoretically. Axial deformability of the corner of the core wall under diagonal lateral earthquake forces was investigated through tests of four L-shaped walls. Confinement details of the corner and extended compressive regions to flange walls ensured very ductile and stable behavior to large inelastic deformations under ultimate high axial compression in skewed bending. Seismic performance of a 12-story hybrid wall system was simulated to be satisfactory under extremely severe earthquake motions from dynamic response analyses based on the test results.

KEYWORDS

Reinforced concrete; core wall; hybrid structure; wall system; bi-directional seismic design; earthquake response analysis; dynamic magnification; shear strength; confinement; varying axial load.

INTRODUCTION

A five-year U.S.-Japan cooperative research program started in 1993 to establish a general seismic design method for hybrid structures, which combine different structural materials, members, or systems. As a part of the program, experimental and analytical investigations on seismic design of hybrid wall structural system have been conducted. The hybrid wall system consists of reinforced concrete coupled core walls and peripheral steel frames. The core walls are supposed to be constructed efficiently using jumping form system and to carry most part of lateral earthquake forces. The steel frames may be designed as nonseismic structure using long spans or an irregular plan. Comprehensive experimental and analytical investigations are being carried out to obtain seismic behavior of the core walls, to develop a rational mathematical macroscopic modeling of the core wall, to simulate earthquake responses of the hybrid wall system and to establish a rational design procedure for the hybrid wall system.

TESTS OF CORE WALLS UNDER VARYING AXIAL LOAD

T-shaped and L-shaped walls were tested under lateral shear and varying axial load simulating responses of the system during an earthquake. The specimens represented lower parts of reinforced concrete coupled core walls in a 12-story prototype structure of hybrid wall system as shown in Fig. 1. Under the lateral loading, especially in the skewed direction of loading, the core wall will be subjected to large amplitude of varying axial load from the beams and the tensile parts. The objective of the tests was to investigate on stiffness, strength and deformability of the walls under varying and high axial compression.

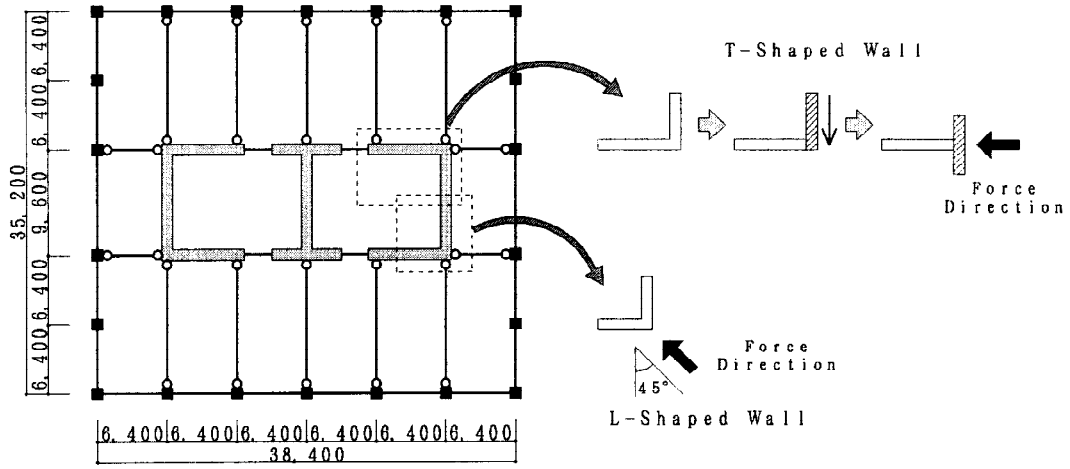

Fig. 1 Prototype 12-story structure of hybrid wall system

Three T-shaped specimens HW-1 through HW-3 were tested as the first phase in 1994, whereas four L-shaped specimens L-1 through L-4 as the second phase in 1995. The specimens were one third scale model. The sectional sizes of T-shaped walls were 20cm thickness, 220cm length, 160cm flange width and 300cm height, as shown in Table 1(a) and Fig. 2. Because the loading for the first phase test is only one-way parallel to the coupling beams, T-shaped model is selected. Reinforcement ratios and loading conditions were varied as listed in Table 1(c). L-shaped walls were tested in the second phase to investigated the effect of confinement on the corner under diagonal lateral loading. The specimens represented only the corner of the wall with webs of 90 cm length and 100cm height, which had the boundary regions well-confined by spiral hoops and sub-ties using ultra-high strength steel(U5.1) as listed in Table 1(b). Only the confinement reinforcement ratios and details of the corner were varied among the four specimens of the L-shaped test series as shown in Fig. 3. The material properties of concrete and reinforcing steel are listed in Table 2.

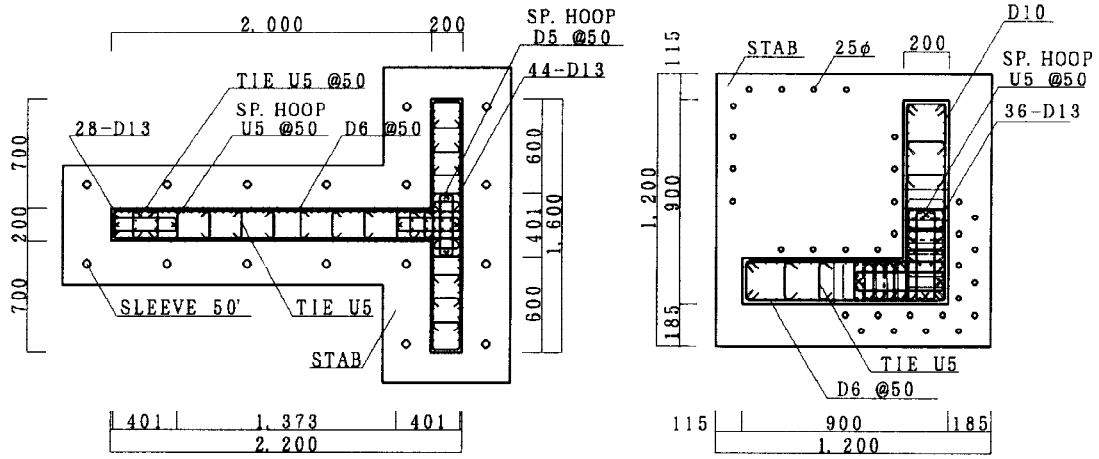

(a) T-shaped walls ***(b) L-shaped walls***

Fig. 2 Reinforcement details of T-shaped and L-shaped wall specimens

Table 1 List of T-shaped and L-shaped wall specimens

(a) Sectional Area (unit in mm)

Series	Specimens	Web Wall	Flange Wall	Height of Wall	Equivalent Loading Height
T-shaped	HW-1～HW-3	200x2200	200x1600	3000	4000
L-shaped	L-1～L-4	200x900	200x900	1000	4000

(b) Boundary Confined Region

Series	Specimen	Region	Area	Main Bar (ratio, $x10^{-2}$)	Confinement U5.1 (ratio, $x10^{-2}$) corner/ boundary in L-series
T-shaped	HW-1～	Web-tip	200x428	28-D13(4.15)	Spiral+4 Sub-tie@50 (0.80)
	HW-3	Flange	200x(428+200)	44-D13(4.26)	2 Spiral+6 Sub-tie@50 (0.80)
L-shaped	L-1	Corner	200x(428+200)	36-D13 (3.64)	2 Sp.+4 tie@50(0.80) / Sp. +4 tie@50(0.80)
	L-2				Sp.+4 tie@50(0.80) / 6 tie@50(0.40)
	L-3				2 Sp.+4 tie@25(1.60) / 6 tie@50(0.40)
	L-4				2 Sp.+4 tie@25(1.60) / 2 tie@100(0.20)

(c) Panel Reinforcement and loading conditions

Specimens	Wall Long. Re.	Wall Lateral Re.	Shear-span-to-depth ratio M/VL (L=2000mm)	Axial Load varied in relation to Shear V	Initial Axial Load No (kN)
HW-1	2-D6@50(0.64)	2-D6@50(0.64)	2.25	170 + 1.5V#	1668
HW-2	2-D10@50(1.42)	2-D6@50(0.64)	2.5, 2.0, 1.75 (to failure)	N0 + 1.0V	
HW-3	2-D10@50(1.42)	2-D6@33(1.06)	2.25	N0 – 0.5V	
L-1～L-4	2-D6@50(0.64)	2-D6@50(0.64)	2.0	N0 + 12V	1470

N0 + 3.0V(1/400)

Table 2 Material properties

(a) Concrete

Series	Age	Elastic Stiffness (MPa)	Compressive Strength σ_B (MPa)
T-shaped	99	27200	35.5
L-shaped	41	32400	35.6
L-shaped	64	32900	36.5

(b) Steel

Series	Nominal Diameter (mm)	Yield Strength (MPa)	Tensile Strength MPa
T-shaped	D6	402	548
	D10	366	518
	D13	367	538
	U5.1	1375	1446
L-shaped	D6	352	527
	D10	385	510
	D13	343	507
	U5.1	1207	1318

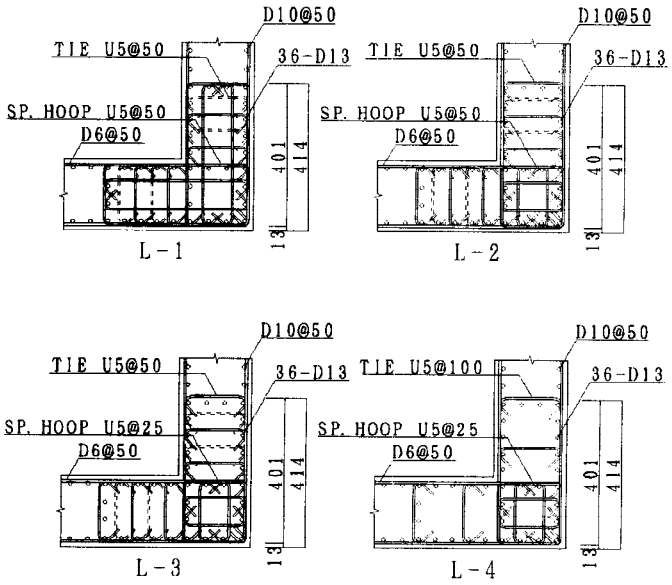

Fig. 3 Details of L-shaped specimens

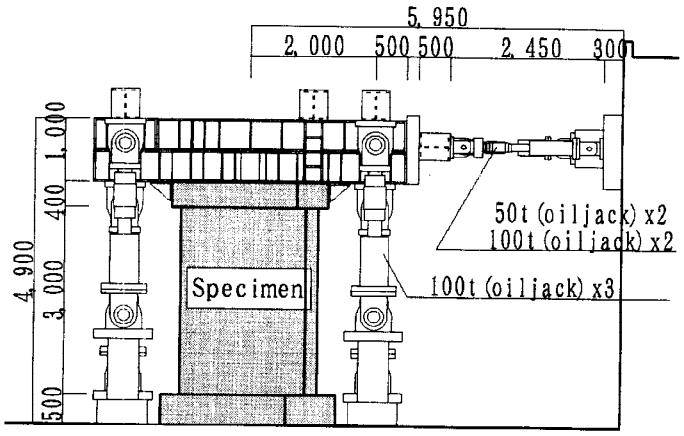

Fig. 4 Loading setup

The walls were subjected to lateral shear, bending moment and axial force using four horizontal and six vertical oil jacks as shown in Fig. 4. The first one cycle reversed at 1/400 and every two cycles at 1/200, 3/400, 1/100, 3/200, 1/50 and 1/30. To simulate varying axial load from the earthquake induced shear in the coupling beams, the axial load N was varied from the initial constant axial load N_0 (= *1668 (kN)* in T-series and *1470 (kN)* in L-series) controlled in proportion to the measured lateral shear V according to the equation: $N = N_0 + \alpha V$. In the specimen HW-1, the constant α was selected as 1.5, as listed in Table 1(c), which was estimated if the coupling beams and wall base yield simultaneously in the prototype structure. However, in the first cycle of 1/400, α was set as 3.0 by mistake. The positive direction in the test was defined as flange compression side and also total axial load in compression. In the specimen HW-2, the constant α was selected as 1.0. In the loading parallel to the coupling beams, positive value of α is expected in the prototype structure. However, in the specimen HW-3 under α of -0.5, large compression was deliberately applied to the tip side of the wall, simulating axial load under skewed diagonal earthquake force. In the second phase, the constant α was selected as 12.0 to simulate high axial compression on the corner due to the skewed lateral earthquake forces.

Constant moment-to-shear ratios were changed among the specimens to control the shear force level at flexural yielding. In the specimens HW-1 and HW-3, shear span-to-depth ratio of 2.25, i.e., equivalent shear span height of 4.5m, was kept constant by applying symmetric bending moment by the vertical jacks. The value was made smaller than expected from static analysis of the prototype structure, so that ductile behavior was to be verified under higher level of shear. In the specimen HW-2, the shear level was increased with deformation level, as shear-span-to-depth ratios of 2.5 within the rotation of 1/200, 2.0 in 1/133, and 1.75 to failure, as listed in Table 1(c), so that the ultimate shear strength could be observed.

WALL TEST RESULTS AND ANALYSES

In the T-shaped test series, different modes of ultimate failure dominated in flexural, in shear, or in axial compression, were observed as intended. The specimen HW-1 under a simulated uni-directional loading condition of the prototype structure remained ductile in flexure until 3 percent drift. The specimen HW-2 under lower moment-to-shear ratios and higher shear failed in web-crushing at about 1 percent drift. The specimen HW-3 was subjected to very large axial compression at a boundary region simulating bi-lateral effects. Though the large compressive strains were measured, well-confined boundary regions enabled ductile behavior until 2 percent drift.

The hysteresis relations between the shear force and the lateral displacement at wall top were shown in Fig. 5. The hysteresis loops of the T-shaped walls would generally be asymmetrical. However, almost symmetrical hysteresis loops were obtained for HW-1 and HW-2. This is due to varying axial load and tensile reinforcement. The amplitudes of varying axial load were ±2038 and ±2009 kN, which almost corresponded to the axial tensile force increment by the incremental reinforcement in the flange region. It may be concluded that the yield force of the tensile reinforcement is twice as effective as the axial load, not only on the strength but also on the stiffness of the wall. Therefore, if the incremental longitudinal reinforcement in the flange, which is tensile under decreasing axial load, is designed as equal to the estimated varying axial load level, it might be expected that the shear forces carried by the tensile and the compressive coupled shear walls would be made equal. However, the shear strength might decrease a little under lower axial load. It might not be reasonable to make equal the shear levels of the tensile and compressive walls.

Small compressive axial strains were observed in the positive direction of HW-1 and HW-2 in spite of larger axial load, which was carried by the flange walls. In HW-3, due to the larger axial compression to the web-tip in the negative direction, large axial strains, about 3 percent at 1 percent drift, were observed. However, overall hysteresis relations were stable because of sufficient confinement reinforcement details at the edges.

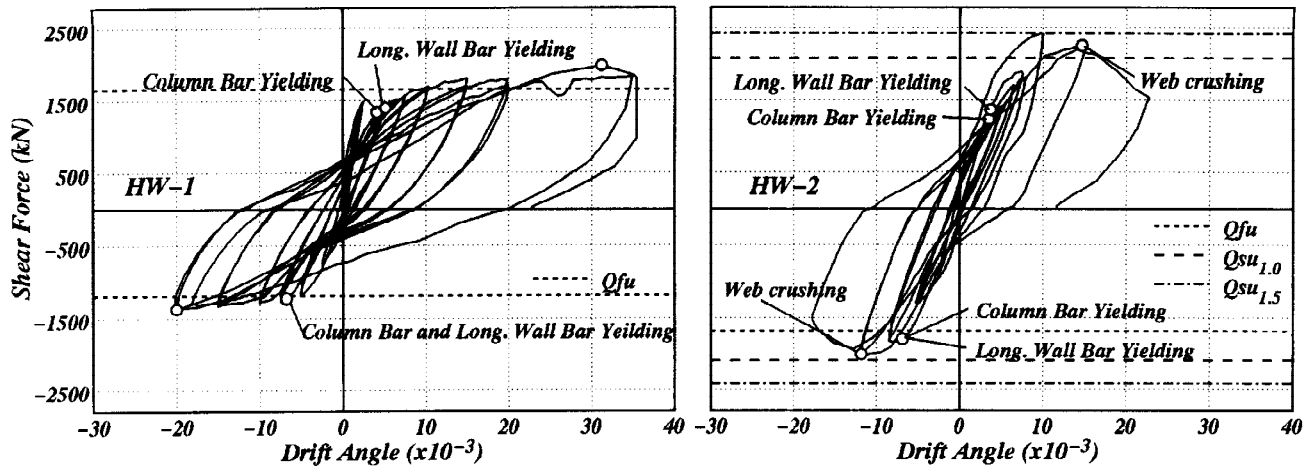

Fig. 5 Observed hysteresis relations in T-series

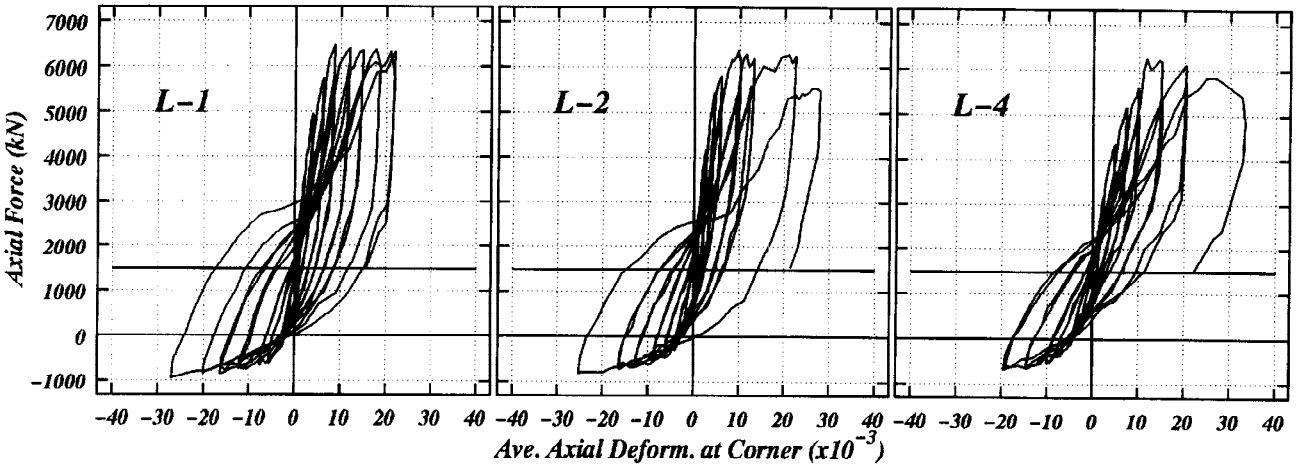

Fig. 6 Averaged axial strains vs. total axial load in L-series

The L-shaped test series simulated high axial compression on the corner of the core wall under skewed loading. Axial strains measured at the corner of L-shaped specimens are shown in Fig. 6. The strains were averaged along total height of the wall. Therefore, the maximum strain is slightly larger than the averaged. The axial load and the measured strain level was investigated by the flexural theory. The axial compressive stress level at ultimate flexural strength in the confined region is may be used as the index for confinement design to ensure ductility. In the AIJ design guidelines(1990), the index for the stress level in core concrete η c is calculated based on the equilibrium of axial stress on assumption that all the compressive force is averaged only in core concrete and longitudinal bars normalized to the strength of concrete σ_B as:

$$\eta_c = \frac{\overline{\sigma}_c}{\sigma_B} = \frac{N + a_t\sigma_y - a_c\sigma_y}{A_{core}\sigma_B} \qquad (1)$$

where, N is the total compressive force to the wall; a_t and a_c is the areas of tensile and compressive longitudinal bars; σ_y is the yield stress of concrete. In the AIJ guidelines, the averaged axial stress is limited as the nominal compressive strength of concrete σ_B, i.e., η_c should be less than or equal to unity.

For the L-shaped specimens, η_c is calculated as 1.3 if the confined area is taken for L-shaped confined area of 174x(200+400) mm^2. Well-confined region for the specimen L-4 is only the corner square of 174x174, for which η c is calculated as 4.5. However, the specimen L-4 was ductile until 1/50. The index might not be appropriate. This is because the axial force could be carried by the extended flange regions, which could

be observed in axial strain distribution measured at the base. The measure strain was compressive even in the edge on the tensile side. If the corner is well confined, the compressive region could extend to unconfined region with slight deterioration in strength.

Ultimate flexural strengths of the T-shaped specimens were calculated based on a flexural theory. To calculate the flexural strengths, the varying axial load level at flexural strength can be determined from the fixed loading rule. The longitudinal reinforcing bars in the flange walls were assumed as fully effective. The observed flexural strengths could fairly be estimated by the design equations based on flexural theory. Shear strength was calculated by the plastic theory combining arch and truss mechanisms. The observed and calculated strengths are listed in Table 3. The calculated strengths are also shown with dashed lines in the hysteresis relations of Fig. 5.

Table 3 Observed and calculated strengths of T-shaped walls

Specimens	*Direction tension side*	*Axial Force on Core* η c	*Maximum*	*Ultimate Flexure*	*Ultimate Shear* $\cot\phi$*=1.0*	*Ultimate Shear* $\cot\phi$*=1.5*
HW-1	*Web-tip (+)*	*1.08*	*1979 (31.2)*	*1659 (1.19)*	*2087 (0.95)*	*2421 (0.82)*
HW-1	*Flange (–)*	*0.59*	*1359 (20.1)*	*1182 (1.15)*	*2087 (0.65)*	*2421 (0.56)*
HW-2	*Web-tip (+)*	*1.08*	*2427 (10.0)*	*2805 (0.79)*	*2087 (1.08)*	*2421 (0.93)*
HW-2	*Flange (–)*	*1.08*	*2009 (18.4)*	*1682 (1.19)*	*2087 (0.96)*	*2421 (0.83)*
HW-3	*Web-tip (+)*	*0.40*	*1257 (15.6)*	*1140 (1.10)*	*3050 (0.41)*	*3808 (0.33)*
HW-3	*Flange (–)*	*2.18*	*2210 (19.6)*	*2109 (1.05)*	*3050 (0.72)*	*3808 (0.58)*

(unit in kN and x0.001 rad.) ϕ*: assumed angle of strut for truss action.*

The shear strengths were observed from the specimen HW-2. The maximum strength of 2427 kN was observed in the positive direction at a lateral drift of 1/100. Obvious shear failure was not observed. In the negative direction of loading right after this a brittle shear failure occurred at a lower strength of 2009 kN. This might be effect on lower axial load on the shear strength. Even after the shear failure in the negative direction the specimen attained higher strength of 2252 kN in the positive direction than that in the negative direction. The effect of axial load on the shear strength was evident which should be investigated further. The calculated shear strengths by assuming $\cot\phi = 1.5$ *and* 1.0 was 2421 kN and 2087 kN. The observed maximum strength could fairly be predicted by a strut and substrut model of $\cot\phi = 1.5$.

EARTHQUAKE RESPONSE ANALYSES OF THE SYSTEM

Earthquake response analyses of the prototype 12-story hybrid wall system were conducted using nonlinear member model of the wall with three line elements(Kabeyasawa, 1983). The structure was idealized as plane frames in the longitudinal direction of coupled shear walls and steel frames. The one-component model and bi-linear hysteresis was used for steel members. The details of the designed structure is given elsewhere(Kabeyasawa, 1995).

The wall model for the dynamic analysis was verified by comparing with the skeletons from the model and the wall test of HW-1. Static push-over analysis of the structure was carried out under lateral load distribution of Japanese design code, as shown in Fig. 7. The prototype structure has about ultimate lateral load-carrying capacity of 0.40 in terms of bases shear coefficient, because the structures is designed according to the requirements of the Japanese design code on the reinforced concrete structures, in the cases of which more than 70 percent of the seismic forces are carried by the shear walls.

Extremely strong motions were used in the dynamic analyses. The accelerations were amplified by two times from the three original accerograms of El Centro (NS, 1940), Hachinohe (EW, 1968) and Tohoku Univ. (NS, 1978) records, which correspond to 1.3 times higher than those currently used in dynamic analyses for special approval seismic design of high-rise buildings in Japan. Original records of 1995

Hyogoken-nanbu earthquake (JMA Kobe and Ohsaka Gas Fukiai station) were also used in the analyses. Maximum dynamic responses of inter-story drifts are shown in Fig. 8. The drift angles are from 0.5 percent to 1.0 percent even under the extreme severe motion except for Fukiai response. The distribution along height of the structure is almost uniform but apparently small in the lower stories, which should be noted to estimate damages to the wall in comparison with the test results.

Maximum dynamic shear forces in the walls normalized by the total weight of the structure are shown in Fig. 9(a). Static shear responses calculated at 1/100 drift were shown in the figure with thick lines. Estimated ultimate shear capacity of the wall is also shown in the figure. The shear capacity was estimated from the ultimate strength of the test specimen HW-2, which was lower in the tensile and higher in the compressive direction.

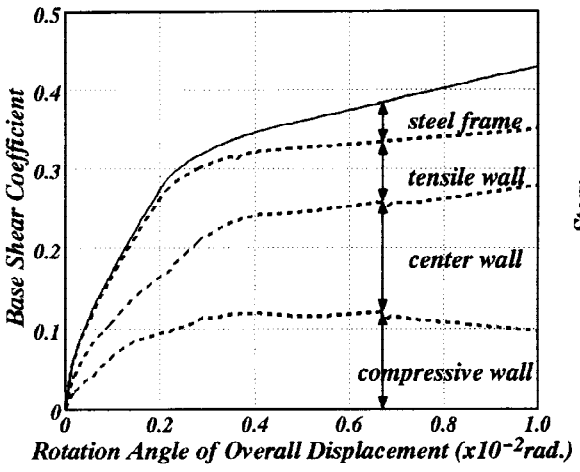

Fig. 7 Static pushover analysis

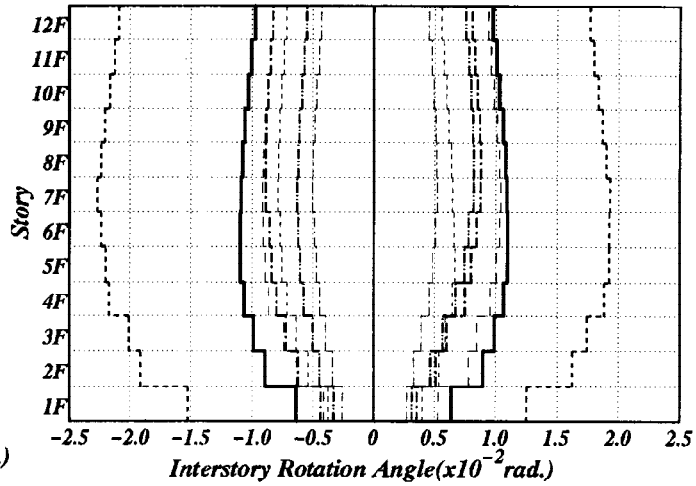

Fig. 8 Maximum displacement responses

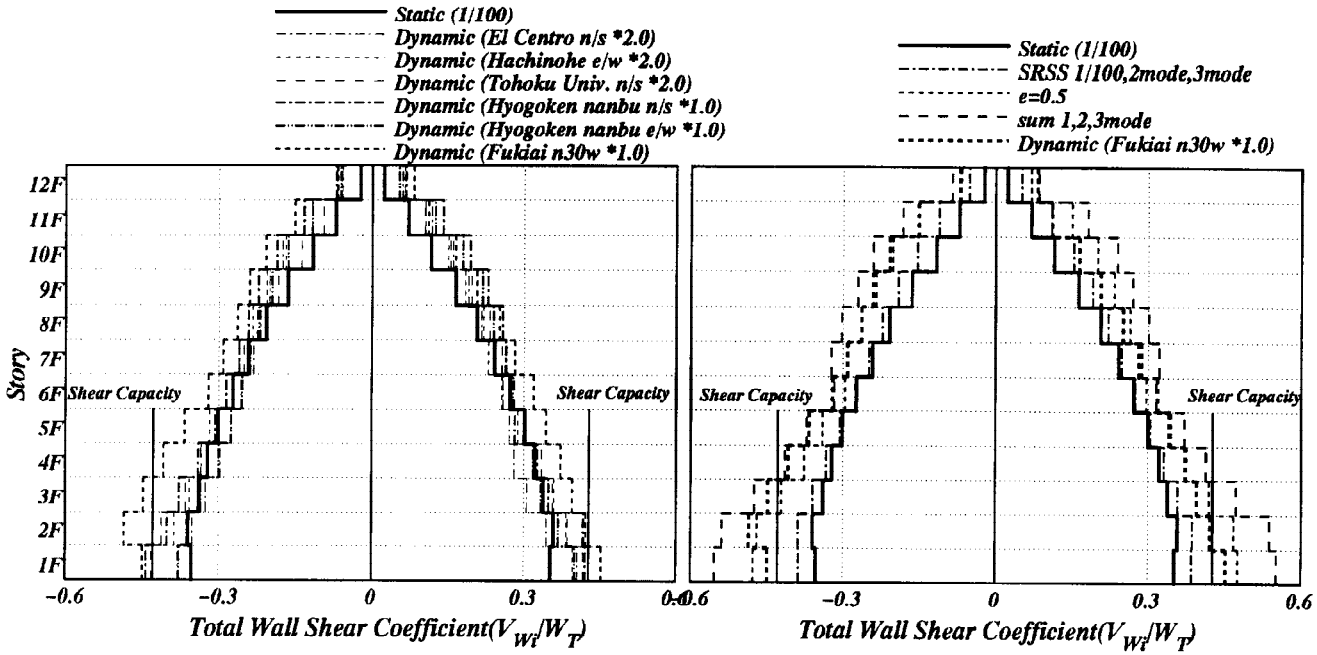

(a) Responses to six records *(b) Fukiai response and estimates*

Fig. 9 Maximum wall shear responses and capacity

The estimated shear capacity is higher than the static response. However, the dynamic wall shear responses are close to or larger than the shear capacity due to the higher mode effects. Dynamic magnification of the responses of maximum shear forces into the wall can roughly be estimated theoretically as the modal sum

of static maximum and elastic higher mode responses(Kabeyasawa, 1987), because the decomposed higher modes generally correspond to elastic magnification. Based on the concept and using acceleration spectra, the maximum responses are formulated as the modal sum of the inelastic basic mode and the elastic higher modes. However, the normal SRSS formula ($e=0$ in eq. (2)) underestimates and the direct sum of all maxima ($e=2$ in eq. (2)) overestimates the maximum shear responses. The following formula including superposition among modes is presented here. Use of $e=1$ gives a fair estimation for the calculated responses as compared for an example of Fukiai response in Fig. 9(b).

$$Q_{Dm} = \sqrt{Q_1^2 + \sum_{j=2}^{n} Q_j^2 + 2e\sum_{j\neq k} Q_j Q_k} \qquad (2)$$

Q_{Dm}: *estimated dynamic shear of* $m-th$ *story*
Q_1: *ultimate static shear under first mode from nonlinear analysis*
Q_j: *shear response of* $j-th$ *higher mode from linear accelerationresponse spectra*

$$= \left(\sum_{i=m}^{n} m_i \beta_j u_{ij} \right) S_{Aj}$$

m_i: *mass of the structure of* $i-th$ *story*
β_m, u_{jm}: *participation factor and mode shape of* $j-th$ *mode*
S_{Aj}: *accelerationspectra of* $j-th$ *mode*

CONCLUSIONS

Ductile hysteretic behavior can be expected from the T-shaped and L-shaped wall tests under extremely high level of shear and varying axial loads due to confinement details and flange wall. The hysteresis shapes of coupled T-shaped walls can be designed as symmetrical taking the equivalent effects of axial load and longitudinal reinforcement. The dynamic wall shear responses might reach the shear capacity of the wall due to dynamic magnification under extremely severe earthquake motions. Theoretical estimation of the dynamic effect presented may be available in the shear design of the walls.

ACKNOWLEDGMENTS

The wall tests and analysis were conducted as a part of U.S.-Japan cooperative research program at Yokohama National University. The authors gratefully acknowledge the contributions of Messrs. K. Aota, H. Arima, Y. Arizono, A. Ishii, R. Yokomatsu, K. Uechi, K. Kikuchi in the experiments.

REFERENCES

Architectural Institute of Japan(1994). *AIJ structural design guidelines for reinforced concrete buildings based on ultimate strength concept (in English).* Architectural Institute of Japan.

Kabeyasawa, T., H. Shiohara, S. Otani and H. Aoyama(1983). Analysis of the Full-Scale Seven-Story Reinforced Concrete Test Structure. Journal of the Faculty of Engineering, The University of Tokyo(B), Vol. XXXVII, No. 2, pp. 431-478.

Kabeyasawa, T.(1987). Ultimate-State Design of Reinforced Concrete Wall-Frame Structures. Proceedings of The Pacific Conference on Earthquake Engineering, New Zealand, Vol. 1, pp. 1-12.

Kabeyasawa, T., Ohkubo, T. and Nakamura, Y.(1995). Tests and Analyses of Reinforced Concrete Core Walls under Varying Axial Load, Pacific Conference on Earthquake Engineering, Melbourne, Vol.2, pp. 145-153.